Application of Southwell Method on the Analysis of Lateral Torsional Buckling Tests on Reinforced Concrete Beams

İlker Kalkan

Civil Engineering Department, Kirikkale University, Kirikkale, 71451 Turkey.
Phone: +90 (318) 357-4242; Fax: +90 (318) 357-2459, ilkerkalkan@yahoo.com,

Abstract — In this study, different versions of the Southwell plot method were applied on the lateral deflection, twisting rotation and load data of slender rectangular reinforced concrete beams, experiencing elastic lateral torsional buckling. Among different versions of the Southwell plot, the Modified (Trahair) Plots produced the critical load estimates in closest agreement with the experimental buckling loads of the beams. The initial geometric imperfection estimates closest to the actual values were obtained from the standard Southwell Plots. The analysis also indicated that the slope of the Southwell plot of a reinforced concrete beam does not change up to 80-90% of the critical load. In the vicinity of buckling and in the post-buckling stage of the test, cracking of concrete caused by the lateral bending and torsional moments in the beam results in the gradual decrease of the slope of the plot.

Index Terms—Southwell Plot; Massey Plot; Meck Plot; Modified Trahair Plot; Lateral torsional buckling, Lateral deflection, Twisting rotation, Modifications to the Southwell plot; Slender reinforced concrete beams.

I.   INTRODUCTION

Southwell (1932) method is a plotting technique, which is used for estimating the critical load and the initial geometric imperfections of a column by using its experimental load and deflection data at loads smaller than the buckling load. According to this method, the lateral deflection (u) vs. deflection-to-load ratio (u/P) plot of a column approaches to a straight line, whose inverse slope and abscissa-intercept are the critical load and the initial lateral imperfection of the column, respectively. Since the experimental measurements at loads smaller than the buckling load are needed, the method eliminates the need for testing a column to failure.

The differential equation governing the flexural buckling of a column with an axial load of P is given as

$$EI \cdot \frac{d^2 u_x}{dx^2} = -P \cdot \left(u_x + u_{ox} \right) \tag{1}$$

where u_{ox} and u_x are the initial lateral deflection and the lateral deflection at a load P of the column at a distance x from the member end; and EI is the flexural rigidity of the column. The lateral deflections of the column at the initial configuration and at a particular load P are assumed to vary as half-sine waves along the beam length. Therefore, the lateral deflections (u_{ox} and u_x) at the distance x are expressed in terms of the midspan lateral deflections (u_o and u) according to the following equations:

$$u_x = u \cdot \sin\left(\pi \cdot x / L \right) \tag{2}$$

$$u_{ox} = u_o \cdot \sin\left(\pi \cdot x / L \right) \tag{3}$$

where L is the span length of the beam. Substituting Equations (2) and (3) into Equation (1), the following equation is obtained:

$$\left(\frac{u}{P} \right) \cdot P_{cr} = u + u_o \tag{4}$$

where P_{cr} is the critical load, which is

$$P_{cr} = \frac{\pi^2 EI}{L^2} \tag{5}$$

Southwell Plot is a natural outcome of Equation (4), which suggests that the slope and u-intercept of the u vs. u/P plot are the critical load (P_{cr}) and the initial lateral imperfection (u_o) of the column, respectively. The following form of Equation (4) is also commonly used for expressing the relationship between the deflection (u) at a certain load and the initial imperfection (u_o):

$$u = \frac{u_o}{P_{cr}/P - 1} \tag{6}$$

Southwell method originally applies to the flexural buckling of columns, which is characterized by the lateral deflection only. On the other hand, a beam undergoes twisting rotations as well as lateral deformations in lateral torsional

buckling (Fig. 1). Therefore, lateral torsional buckling is characterized by the twisting rotation (φ) in addition to the lateral deflection (u). Different from column buckling, where a single Southwell Plot of the deflection (u) vs. the deflection-to-load ratio (u/P) is needed, two Southwell plots are used in lateral torsional buckling to include the lateral deflection, twist and load data.
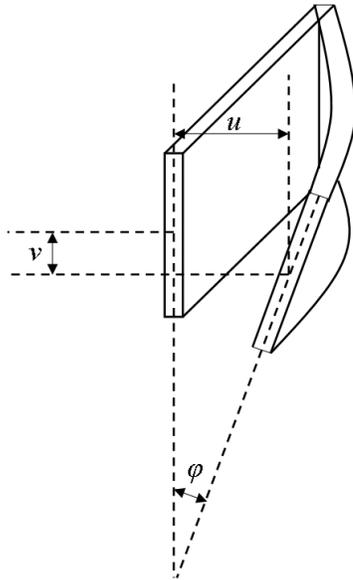

Fig. 1. Lateral torsional buckling

Previously, Dumont and Hill (1940), Gregory (1960), and Cheng and Yura (1988) showed that the standard version of the Southwell Plots, meaning the u/P vs. u and φ/P vs. φ plots, accurately estimate the critical loads of lateral torsional buckling of beams. The standard Southwell plots for the lateral deflection and twisting rotation of a beam are expressed by Equation (6) and Equation (7), respectively.

$$\phi = \frac{\phi_o}{P_{cr}/P - 1} \tag{7}$$

where φ_o and φ are the initial midspan twisting angle and the midspan twisting angle at a particular load P, respectively; and P is the applied transverse load.

Meck (1977) carried out an analytical study, in which he showed that a different version of the Southwell Plots should be used instead of the standard version. Accordingly, u/P should be plotted against φ and φ/P should be plotted against u. The theoretical background for the Meck plots is based on the application of Southwell theory to the case of lateral torsional buckling. The differential equations governing the lateral bending and torsion, involved in lateral torsional buckling, are given in Equations (8) and (9), respectively, for a slender beam (negligible warping rigidity) with constant bending moment M over the span:

$$EI_y \cdot \frac{d^2 u_x}{dx^2} = M \cdot (\phi_x + \phi_{ox}) \tag{8}$$

$$GC \cdot \frac{d\phi_x}{dx} = -M \cdot \left(\frac{du_x}{dx} + \frac{du_{ox}}{dx} \right) \tag{9}$$

where GC and EI_y are the torsional and minor-axis flexural rigidities of the beam, respectively; u_x and φ_x are the lateral centroidal deflection and the angle of twist of the beam at a distance x from the beam end; and u_{ox} and φ_{ox} are the initial lateral centroidal imperfection and the initial twisting angle of the beam at a distance x from the beam end. The lateral deflection and twisting rotation of the beam are assumed to vary as half-sine waves along the length of the beam, leading to the following equations:

$$u_x = -u \cdot \sin\left(\pi \cdot x / L \right) \tag{10}$$

$$u_{ox} = -u_o \cdot \sin\left(\pi \cdot x / L \right) \tag{11}$$

$$\phi_x = \phi \cdot \sin\left(\pi \cdot x / L \right) \tag{12}$$

$$\phi_{ox} = \phi_o \cdot \sin\left(\pi \cdot x / L \right) \tag{13}$$

where φ, φ_o, u and u_o correspond to the midspan of the beam. Substituting Equations (10)-(13) into Equations (8) and (9), the equations setting the stage for Meck plots are obtained:

$$\alpha \cdot \left(\frac{u}{M} \right) = \phi + \phi_o \tag{14}$$

$$\beta \left(\frac{\phi}{M} \right) = u + u_o \tag{15}$$

where α and β are obtained from the following equations:

$$\alpha = \frac{\pi^2 \cdot EI_y}{L^2} \tag{16}$$

$$\beta = GC \tag{17}$$

Finally, the critical moment of the beam is

$$M_{cr} = \sqrt{\alpha \cdot \beta} = \frac{\pi}{L} \cdot \sqrt{EI_y \cdot GC} \tag{18}$$

Equations (14) and (15) indicate that the square root of the product of inverse slopes of the u vs. φ/M and φ vs. u/M graphs gives the critical moment (or load) of the beam. The applied moment M in Equations (14) and (15) can be replaced

with the applied load P, considering a beam subjected to transverse loading at an arbitrary point along the span.

Another modification to the standard version was proposed by Massey (1963), who found out that the term P in the Southwell Plots should be replaced with P^2, meaning that u and φ should be plotted against u/P^2 and φ/P^2, respectively. The inverse slope of each of these plots gives the square of the critical load P_{cr}^2. Assuming that the beam does not have an initial twisting angle ($\varphi_o=0$), φ can be eliminated from Equations (14) and (15) and a single equation is obtained:

$$\alpha \cdot \beta \cdot \left(\frac{u}{M^2}\right) = \sqrt{M_{cr}} \cdot \left(\frac{u}{M^2}\right) = u + u_o \qquad (19)$$

Similarly, u can be eliminated from Equations (14) and (15), by assuming that the beam has no initial lateral imperfection ($u_o=0$):

$$\alpha \cdot \beta \cdot \left(\frac{\phi}{M^2}\right) = \sqrt{M_{cr}} \cdot \left(\frac{\phi}{M^2}\right) = \phi + \phi_o \qquad (20)$$

Equations (19) and (20) suggest that the critical moment (or load) of a beam is the square root of the inverse slope of u vs. u/M^2 or φ vs. φ/M^2 graph if the beam has only one type of initial geometric imperfection ($\varphi_o=0$ or $u_o=0$).

Stratford and Burgoyne (1999) proposed the use of u vs. u/P^2 plots for investigating the lateral stability of slender precast concrete girders, based on the study of Allen and Bulson (1980). Finally, Trahair (1969) proposed the use of a plot of deflection vs. the product of load and deflection, known as the Modified Plot (u vs. $P.u$ and φ vs. $P.\varphi$). The slope of the Modified Plot is the critical load of the beam. By multiplying both sides of Equation (4) by the applied load P, the equation setting the stage for the Modified Plot is obtained:

$$(u \cdot P) = u \cdot P_{cr} - u_o \cdot P \qquad (21)$$

Similarly,

$$(\phi \cdot P) = \phi \cdot P_{cr} - \phi_o \cdot P \qquad (22)$$

Equations (21) and (22) suggest that the major difference of the Modified Plot from the other versions of the Southwell Plot is that the abscissa-intercept of the Modified Plot does not give the initial geometric imperfection of the beam.

Mandal and Calladine (2002) examined the standard version and the modified versions of the Southwell plots and reached significant conclusions. In this study, it was shown that the lateral deflection (u) and the twisting rotation (φ) of a beam are proportional to each other, and therefore, there is a direct coupling between them after the initial stages of loading. Consequently, the critical loads obtained from the standard Southwell Plots are in close agreement with the critical loads obtained from the Meck Plots. Furthermore, Mandal and Calladine (2002) analytically showed that Massey Plots are applicable only to the beams with only one kind of

initial imperfection. To be more specific, the u vs. u/P^2 plot accurately estimates the critical load of a beam only if the beam does not have an initial angle of twist and the φ vs. φ/P^2 plot closely predicts the critical load of a beam when the beam has zero initial lateral centroid deflection. Mandal and Calladine (2002) also found out that in Massey Plots, the initial data points corresponding to the initial stages of loading lie further away from the eventual straight line formed by the remaining data points, compared to the other versions of the Southwell plot.

Cheng and Yura (1988) carried out lateral buckling tests on coped steel beams. They used both the Southwell Plots and Meck Plots to determine the critical loads of the specimens. Since they found out that both versions gave almost the same results, only the critical loads from the Southwell Plots were reported.

Cheng and Yura (1988) stated that the distortions in some of their specimens affected the critical load values obtained from the Southwell plot with the twist data. Since the plot with the lateral deflection data was considered more reliable, the critical load values reported in this study were obtained from the plots with the lateral deflection data.

Attard (1983) applied the Southwell, Modified and Massey plotting techniques on the analysis of lateral torsional buckling of doubly symmetric beams and compared the plots to the final element results. The study led to the conclusion that the Southwell Plot was superior to the other plots for the determination of the critical load and initial geometric imperfections.

II.   RESEARCH SIGNIFICANCE

The Southwell, Modified, Meck and Massey plotting techniques were previously applied on the analysis of lateral torsional buckling of beams of homogeneous, isotropic and linearly elastic material, such as the elastic lateral torsional buckling of steel and aluminum beams. There is a clear need to apply the method on the analysis of lateral torsional buckling of reinforced concrete beams, considering the nonhomogeneous and anisotropic nature of reinforced concrete; the material nonlinearities of concrete and reinforcing steel; and cracking of concrete. In the present study, the inelasticity of concrete and steel is eliminated by considering the experimental data of reinforced concrete beams, undergoing elastic lateral torsional buckling.

III. APPLICATION OF THE METHOD TO THE EXPERIMENTAL DATA

In the present study, the standard Southwell method and the modified versions of the method (Modified, Meck and Massey) are applied to the experimental data on lateral torsional buckling of reinforced concrete beams obtained by Kalkan (2009). Kalkan (2009) tested rectangular reinforced concrete beams with the nominal dimensions and cross-sectional details shown in Fig. 2. The beams were subjected to

a concentrated load at midspan and simply-supported in and out of plane at the ends (Fig. 3). Kalkan (2009) reported that all of the specimens tested in the experimental program failed by elastic lateral torsional buckling. Southwell method is only applicable to the elastic buckling. Therefore, the experimental data obtained by Kalkan (2009) can be analyzed by the Southwell method and by its modified versions.
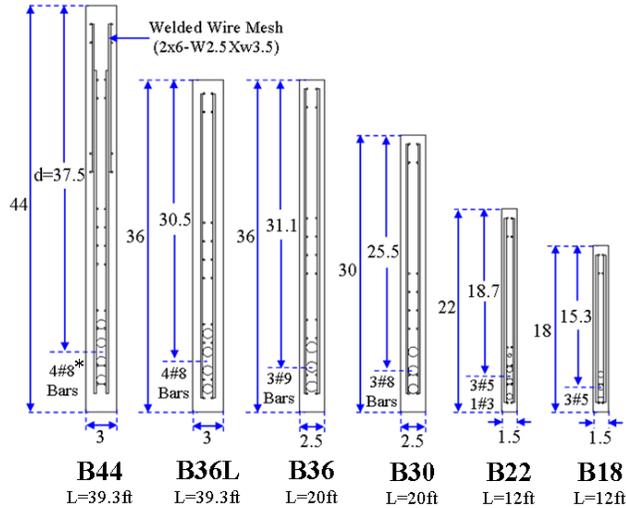
Fig. 2. Nominal dimensions and cross-sectional details of the specimens (All dimensions are in inches, unless otherwise stated)
The bar sizes are in US customary units. The SI equivalents are: #9 = M29; #8 = M25; #5 = M16; and #3 = M10.
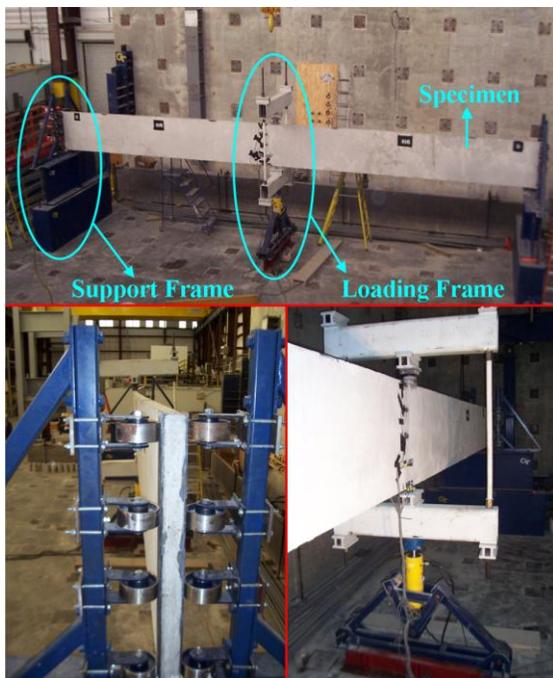

**Fig. 3**. Experimental setup used by Kalkan (2009)

Figs. 4 and 5 illustrate the Southwell Plots for the lateral deflection and twist data of the Specimen B36L-2 tested by Kalkan (2009). Fig. 6 depicts the Meck Plots and Figs. 7 and 8 illustrate the Massey Plots for the lateral deflection and twist data, respectively. Finally, Figs. 9 and 10 illustrate the

Modified Plots for the lateral deflection and twist data, respectively.

Similar to the findings of Cheng and Yura (1988), the present study depicted that the Southwell Plots including the twist data are more complicated to analyze due to the large scatter of the data points caused by the distortions in the specimens, particularly at and around midspan, where the load was applied in the study of Kalkan (2009). The plots in Figs. 5, 6, 8 and 10, which include the twist data, have larger scatter than the plots in Figs. 4, 7 and 9, which incorporate solely the lateral deflection data. In all of the plots, the initial points corresponding to the initial stages of loading do not lie on the straight line formed by the remaining points corresponding to the further stages of loading. The greater dispersion of the initial points from the eventual straight line was explained by Cheng and Yura (1988) with the experimental errors and the small initial restraints in the test setup, which are more pronounced at low load levels.
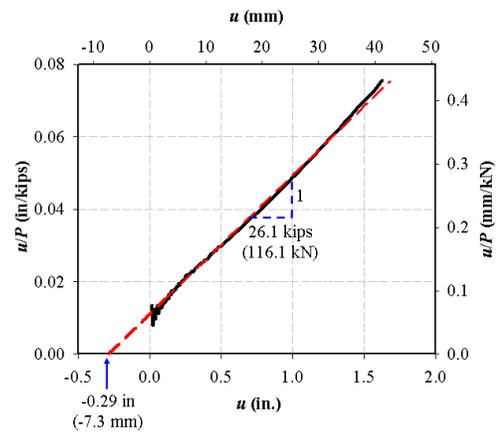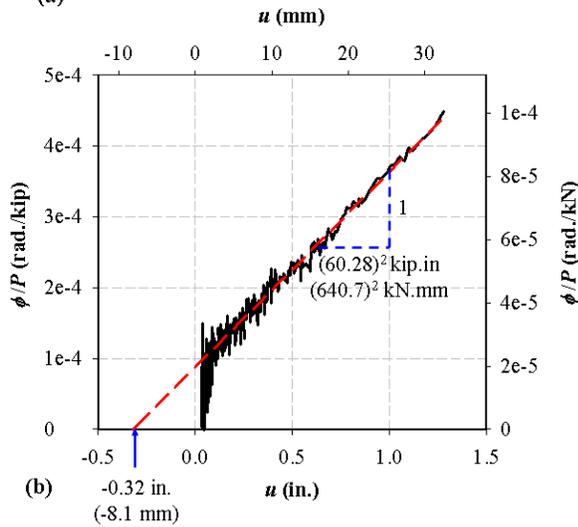

Fig. 4. Southwell Plot for the lateral deflection data of Specimen B36L-2 tested by Kalkan (2009)
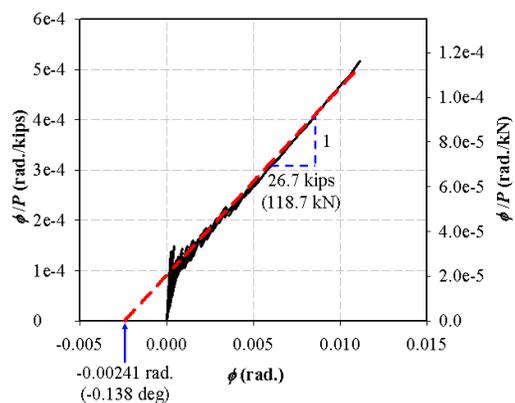
Fig. 5. Southwell Plot for the twisting rotation data of Specimen B36L-2 tested by Kalkan (2009)

(a)

-0.00230 rad.
(-0.132 deg.)

Fig. 8. Massey Plot for the twisting rotation data of Specimen B36L-2 tested by Kalkan (2009)

(b) -0.32 in.
(-8.1 mm)
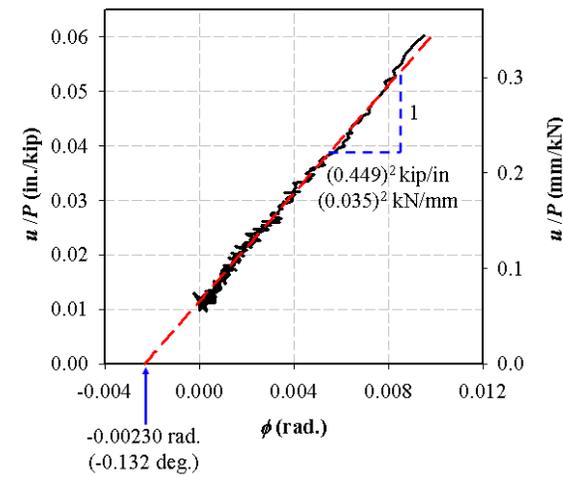
P_{cr} = 0.449 x 60.28=27.1 kips (120.4 kN)

Fig. 6. Meck Plots of Specimen B36L-2 tested by Kalkan (2009): (a) φ *vs.* u/P plot; and (b) u *vs.* φ /P plot.

Fig. 9. Modified Plot for the lateral deflection data of Specimen B36L-2 tested by Kalkan (2009)
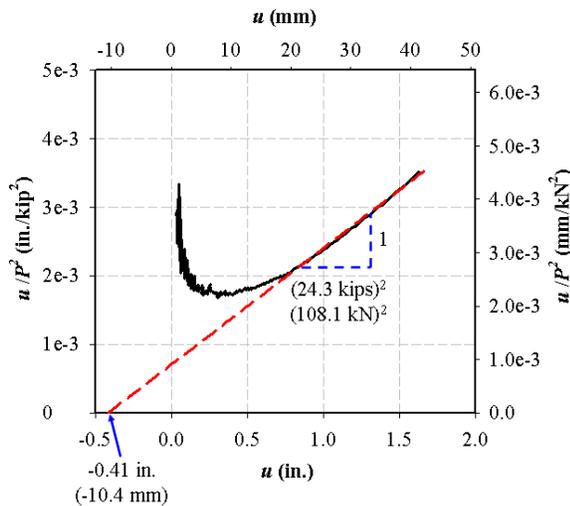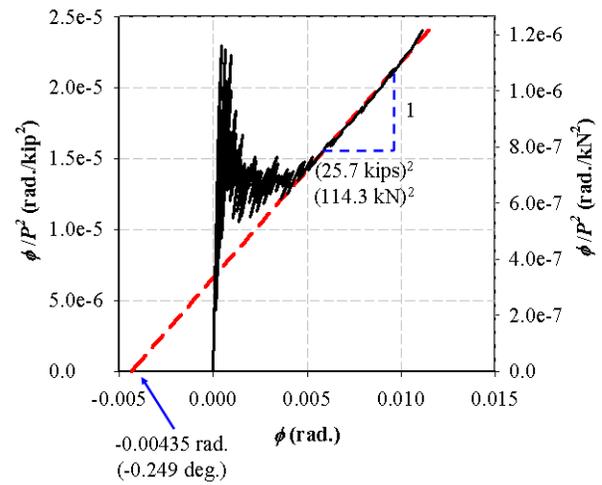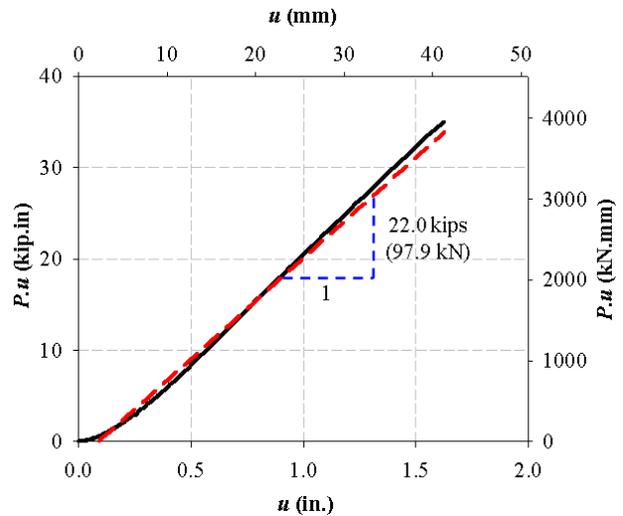

-0.41 in.
(-10.4 mm)

Fig. 7. Massey Plot for the lateral deflection data of Specimen B36L-2 tested by Kalkan (2009)
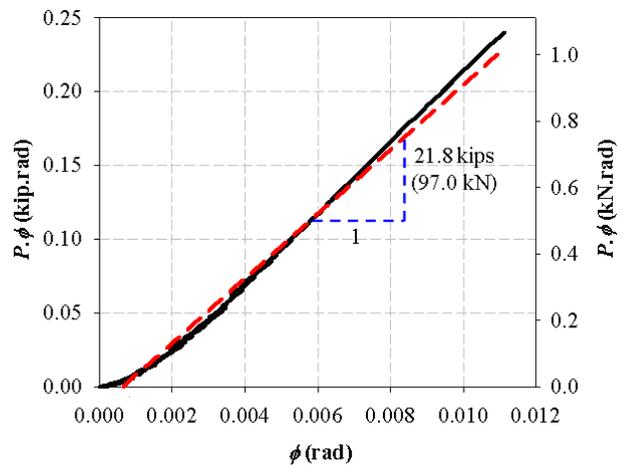
Fig. 10. Modified Plot for the twist data of Specimen B36L-2 tested by Kalkan (2009)

Modified Plots are superior to the Southwell, Meck and Massey Plots in that the initial data points are less scattered, and therefore, more data points lie on the straight line. The Massey Plots in Figs. 7 and 8 verify the findings of Mandal and Calladine (2002). The initial data points lie further away from the eventual straight line compared to the other versions of the Southwell Plots.

Table 1 presents the buckling loads of the specimens tested by Kalkan (2009) together with the critical load estimates obtained from different versions of the Southwell plot. The columns in the table corresponding to the Modified, Meck and Massey Plots are split into two sub-columns, one corresponding to the lateral deflection (u) data and the other corresponding to the twist (φ) data. The estimated-to-experimental critical load ratios are also presented in the table.

The critical load estimates in closest agreement with the experimental buckling loads were obtained from the Modified Plots incorporating the lateral deflection data. The estimated-to-experimental critical load ratios corresponding to this type of plot were in the range of 0.99-1.21 with a mean value of 1.08 and a percent coefficient of variation of 7.8. The Southwell Plot with the twist data, the Massey Plots and the Meck Plots generally overestimated the buckling loads of the specimens. With the exception of Massey Plots, the plots with lateral deflection data produced estimates closer to the test loads than the plots with twist data. This might be caused by the possible distortions in the specimens, which affected the twisting angle values measured in the experiments.

Table 1 – Critical loads from different versions of Southwell plot compared to the experimental buckling loads of the specimens tested by Kalkan (2009)

Beam	Test Buckling Load, P_{exp} kips (kN)	Estimated Critical Load, P_{cr} kips (kN)														
		Modified				Southwell				Meck		Massey			
		Lateral Deflection		Twist		Lateral Deflection		Twist				Lateral Deflection		Twist	
		P_{tl}	P_{tl}/P_{exp}	P_{tt}	P_{tt}/P_{exp}	P_{sl}	P_{sl}/P_{exp}	P_{st}	P_{st}/P_{exp}	P_{meck}	P_{meck}/P_{exp}	P_{ml}	P_{ml}/P_{exp}	P_{mt}	P_{mt}/P_{exp}
B36	39.2 (174.4)	39.8 (177.0)	1.02	41.5 (184.6)	1.06	39.7 (176.8)	1.01	41.8 (185.8)	1.07	41.6 (185.1)	1.06	39.9 (177.5)	1.02	41.6 (185.0)	1.06
B30	22.0 (97.8)	24.2 (107.6)	1.10	24.2 (107.6)	1.10	21.1 (93.9)	0.96	28.5 (126.8)	1.30	34.5 (153.5)	1.57	21.3 (94.8)	0.97	28.1 (125.0)	1.28
B22-1	8.7 (38.7)	10.5 (46.7)	1.21	9.4 (41.8)	1.08	12.0 (53.4)	1.38	10.7 (47.8)	1.23	14.5 (64.5)	1.67	12.4 (55.2)	1.43	9.8 (43.5)	1.13
B18-2	12.0 (53.4)	14.4 (64.0)	1.20	12.1 (53.8)	1.01	14.4 (64.2)	1.20	12.0 (53.3)	1.00	20.1 (89.7)	1.68	12.2 (54.4)	1.02	12.1 (53.8)	1.01
B44-1	15.2 (67.6)	16.0 (71.2)	1.05	17.4 (77.4)	1.14	15.9 (70.8)	1.05	18.7 (83.2)	1.23	18.7 (83.2)	1.23	19.6 (87.2)	1.29	17.0 (76.0)	1.12
B44-2	12.1 (53.8)	12.8 (56.9)	1.06	14.5 (64.5)	1.20	10.7 (47.7)	0.88	12.2 (54.4)	1.01	11.6 (51.6)	0.96	15.4 (68.5)	1.27	11.0 (48.9)	0.91
B36L-1	13.5 (60.0)	13.3 (59.2)	0.99	15.4 (68.5)	1.14	15.5 (68.7)	1.15	19.1 (84.9)	1.41	18.1 (80.6)	1.34	20.4 (90.8)	1.51	16.0 (71.3)	1.19
B36L-2	21.6 (96.1)	22.0 (97.9)	1.02	21.8 (97.0)	1.01	26.1 (116.1)	1.21	26.7 (118.7)	1.24	27.1 (120.4)	1.25	24.3 (108.1)	1.13	25.7 (114.3)	1.19
Sample Mean			1.08		1.09		1.10		1.19		1.34		1.20		1.11
Standard Deviation			0.08		0.07		0.15		0.14		0.27		0.20		0.12
% COV			7.8		6.2		13.5		11.6		20.1		16.8		10.4

Based on the study of Yura (1970), the Southwell plot of a beam should include the test data up to at least 70% of the critical load (P_{cr}) for reliable critical load estimates. Figs. 4-10 include the experimental load and deflection measurements of Specimen B36L-2 up to more than $0.70P_{cr}$.

Reinforced concrete differs from other types of construction materials, such as steel and aluminum, in that concrete cracks when it is subjected to tensile stresses. Due to the cracking of concrete, the slope of the Southwell plot changes with the increasing load. Fig. 11 illustrates the entire Southwell plot of Specimen B36L-2, including the portion of the curve corresponding to the post-buckling stage of the beam.

By examining the experimental data obtained by Kalkan (2009), it was concluded that the slope of the Southwell plot generally does not change up to 80-90% of the buckling load in reinforced concrete beams. Beyond this load level, flexural cracks form in the beam due to the increase in the lateral bending moments. Once the beam

buckles, rapid and excessive lateral deformations and twisting rotations take place and the beam undergoes diagonal tension cracking from torsion in addition to the vertical flexural cracking from lateral bending. The formation of different forms of cracks reduces the rigidity of the beam, and therefore, the slope of the Southwell plot decreases close to the instant of buckling and after buckling. The Southwell plot in Fig. 11 is approximated to a series of linear segments, indicating the gradual decrease in the slope due to the cracking of concrete right before and after buckling. The slope of the first linear segment is in closer agreement with the buckling load of the beam. Consequently, the slope of the first segment was taken into consideration in each Southwell plot to obtain the critical load estimates tabulated in Table 1.
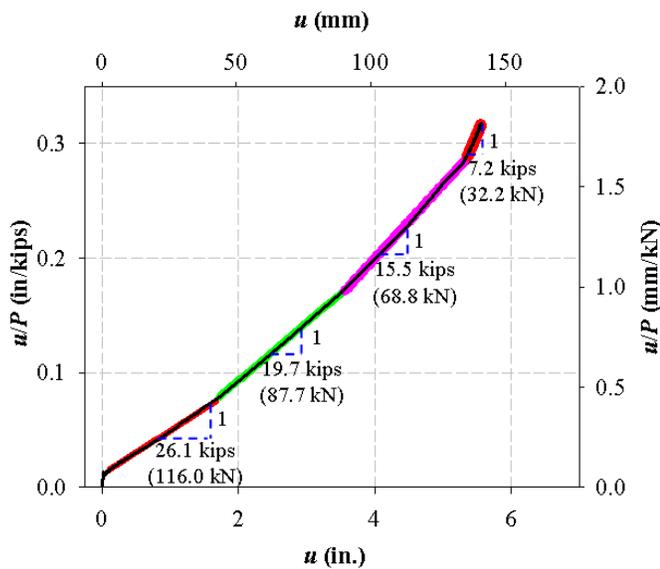

Fig. 9. The entire Southwell plot of Specimen B36L-2 for the lateral deflection measurements

Another advantage of the Southwell plot is that it provides an estimate for the initial geometric imperfections of a beam. In the plot, the absolute value of the intercept of the initial straight line on the abscissa is the initial geometric imperfection of the beam, with the exception of the Modified Plot (Trahair Plot), in which the intercept is $u_o.P$ or $\varphi_o.P$, as given in Equations (21) and (22). The x-intercept of the line in each of Figs. 4, 6(b), and 7 gives the initial lateral centroid deflection of Specimen B36L-2 at midspan, while the x-intercept of the line in each of Figs. 5, 6(a), and 8 gives the initial midspan twisting angle. Tables 2 and 3 tabulate the initial geometric imperfections of the specimens obtained from three versions of the Southwell plot together with the measured imperfection values, reported by Kalkan (2009). Different from Table 1, the initial imperfections of Specimen B22-1 are not given in Tables 2 and 3, since the measured imperfection values belonging to this specimen were not reported by Kalkan (2009).

Tables 2 and 3 indicate that the initial imperfection estimates from the standard Southwell plot are in closest agreement with the measured values reported by Kalkan (2009). The Massey plots generally overestimated the imperfections, while the Meck Plots provided good estimates for the initial lateral centroid imperfections of the specimens.

Kalkan (2009) found out that the lateral stability of reinforced concrete beams is greatly influenced by the initial geometric imperfections. Therefore, the accurate estimation of the imperfections is of great importance in the evaluation of the stability of a reinforced concrete beam. Based on the values tabulated in Tables 2 and 3, the standard Southwell plot is recommended to be used for the estimation of the initial geometric imperfections of a reinforced concrete beam in case the actual imperfections of the beam are not known. The use of the imperfection values from the Massey Plots may cause overestimation or underestimation of the buckling load and the pre-buckling out-of-plane deformations of a reinforced concrete beam.

IV. CONCLUSIONS

Based on the study presented in this paper, the following conclusions are drawn:

- The critical loads of reinforced concrete beams are closely estimated by the Southwell, Modified, Meck and Massey Plots.
- The data points in the plots with twist data are more scattered due to the distortions in slender reinforced concrete beams.
- Among various versions of Southwell plot, the Modified Plot with lateral deflection data produces the critical load estimates in closest agreement with the experimental buckling loads of reinforced concrete beams. The Southwell Plot produces estimates closer to the experimental buckling loads compared to the Meck and Massey Plots.
- The initial points in each plot lie further away from the straight line formed by the majority of the points. The deviation of the initial points from the straight line is caused by the tolerance errors in the test setup, which become less influential as the load increases.
- The initial points are more scattered and they have greater deviations from the straight line in the Massey's version of the plots, which makes the determination of a straight line more complicated.

Table 2 – Initial lateral centroid deflections at midspan of the specimens tested by Kalkan (2009) and the estimated-to-measured imperfection ratios

Beam	Measured Lateral Centroid Imperfection, u_{om} in (mm)	Estimated Initial Lateral Centroid Imperfection, in (mm)					
		Southwell		Meck		Massey	
		u_{os}	u_{os}/u_{om}	u_{omeck}	u_{omeck}/u_{om}	u_{omas}	u_{omas}/φ_{om}
B36	0.19 (4.8)	0.06 (1.5)	0.32	0.20 (5.2)	1.05	0.07 (1.8)	0.37
B30	0.56 (14.3)	0.54 (13.8)	0.96	0.22 (5.7)	0.39	1.80 (45.7)	3.21
B18-2	0.38 (9.6)	0.23 (5.8)	0.61	0.43 (10.9)	1.13	0.28 (7.1)	0.74
B44-1	0.72 (18.2)	0.30 (7.6)	0.42	0.87 (22.1)	1.21	1.50 (25.4)	2.08
B44-2	0.88 (22.3)	0.36 (9.2)	0.41	0.54 (13.6)	0.61	1.39 (35.4)	1.58
B36L-1	0.56 (14.3)	0.43 (10.9)	0.77	1.41 (35.9)	2.52	2.25 (57.2)	4.02
B36L-2	0.19 (4.8)	0.29 (7.3)	1.53	0.32 (8.1)	1.68	0.41 (10.4)	2.16
Sample Mean			0.72		1.23		2.02
Standard Deviation			0.39		0.71		1.29
% COV			54.9		57.4		63.9

Table 3 – Initial midspan twisting angles of the specimens tested by Kalkan (2009) and the estimated-to-measured imperfection ratios

Beam	Measured Initial Angle of Twist, φ_{om} rad (degrees)	Estimated Initial Angle of Twist, rad (degrees)					
		Southwell		Meck		Massey	
		φ_{os}	$\varphi_{os}/\varphi_{om}$	φ_{omeck}	$\varphi_{omeck}/\varphi_{om}$	φ_{omas}	$\varphi_{omas}/\varphi_{om}$
B36	0.0017 (0.10)	0.0007 (0.04)	0.41	0.0015 (0.08)	0.88	0.0017 (0.10)	1.00
B30	0.0042 (0.24)	0.0043 (0.25)	1.02	0.0233 (1.33)	5.55	0.0095 (0.54)	2.26
B18-2	0	0.0001 (0.01)	-	0.0050 (0.28)	-	0.0004 (0.02)	-
B44-1	0.0085 (0.49)	0.0028 (0.16)	0.33	0.0010 (0.06)	0.12	0.0032 (0.18)	0.38
B44-2	0.0028 (0.16)	0.0024 (0.14)	0.86	0.0004 (0.02)	0.14	0.0144 (0.83)	5.14
B36L-1	0.0034 (0.20)	0.0038 (0.22)	1.12	0.0004 (0.02)	0.12	0.0052 (0.30)	1.53
B36L-2	0.0017 (0.10)	0.0024 (0.14)	1.41	0.0023 (0.13)	1.35	0.0044 (0.25)	2.59
Sample Mean			0.86		1.36		2.15
Standard Deviation			0.42		2.11		1.67
% COV			48.9		155.3		77.9

- The initial data points in Modified Plots are least scattered in comparison with the initial data points in Southwell, Meck and Massey Plots. In other words, the Modified Plots have larger range of approximate linearity compared to the Southwell, Meck and Massey Plots.
- When the experimental data of the post-buckling stage of the test is included, the Southwell plot of a reinforced concrete beam can be approximated to a series of lines with decreasing slopes. The initial line ends at 80-90% of the critical load, beyond which the slope decreases due to the diagonal tension and vertical flexural cracking of concrete originating from torsion and lateral bending, respectively. The critical load estimate

obtained from the initial line is generally in closer agreement with the actual buckling load of the beam.

- Among different versions of the Southwell plot, the initial geometric imperfection estimates from the standard version are in closest agreement with the measured values. In general, the estimates from Massey Plots are considerably greater than the actual values, while the initial lateral imperfection estimates from Meck Plots agree well with the measured values.

V. NOTATION

EI	:	Flexural rigidity
P	:	Applied load
P_{cr}	:	Critical load
P_{exp}	:	Experimental buckling load
P_{ml}	:	Critical load estimate from the Massey Plot with lateral deflection data
P_{mt}	:	Critical load estimate from the Massey Plot with twist data
P_{meck}	:	Critical load estimate from the Meck Plots
P_{sl}	:	Critical load estimate from the Southwell Plot with lateral deflection data
P_{st}	:	Critical load estimate from the Southwell Plot with twist data
P_{tl}	:	Critical load estimate from the Modified (Trahair) Plot with lateral deflection data
P_{tt}	:	Critical load estimate from the Modified (Trahair) Plot with twist data
u	:	Lateral (Out-of-plane) deflection at midspan
u'	:	Lateral deflection of the member at a distance x from the member end
u_o	:	Initial lateral centroid imperfection at midspan
u_o'	:	Initial lateral imperfection of the member at a distance x from the member end
u_{om}	:	Measured initial lateral centroid imperfection at midspan
u_{omas}	:	Initial lateral centroid imperfection estimate obtained from the Massey Plot
u_{omeck}	:	Initial lateral centroid imperfection estimate obtained from the Meck Plot
u_{os}	:	Initial lateral centroid imperfection estimate obtained from the standard Southwell Plot
v	:	Vertical (In-plane) centroid deflection at midspan
φ	:	Angle of twist at midspan
φ_o	:	Initial twisting angle at midspan
φ_{om}	:	Measured initial midspan twisting angle
φ_{omas}	:	Initial midspan twisting angle estimate obtained from the Massey Plot
φ_{omeck}	:	Initial midspan twisting angle estimate obtained from the Meck Plot

Attard, M. M. (1983), "Extrapolation Techniques for Buckling Loads", *Journal of Structural Engineering, ASCE,* Vol. 109, No. 4, pp. 926-935.

Cheng, J. J. R. and Yura, A. Y. (1988), "Lateral Buckling Tests on Coped Steel Beams", *Journal of Structural Engineering*, *ASCE*, Vol. 114, No. 1, pp. 16-30.

Dumont, C. and Hill, H. N. (1940), "The Lateral Stability of Equal Flanged Aluminum-Alloy I Beams Subjected to Pure Bending", *N.A.C.A.* TN 770.

Gregory, M. (1960), "The Application of the Southwell Plot on Strains to Problems of Elastic Instability of Framed Structures, where Buckling of Members in Torsion and Flexure Occurs", *Australian Journal of Applied Science*, Vol. 11, pp. 49-64.

Kalkan, I. (2009), "Lateral Torsional Buckling of Rectangular Reinforced Concrete Beams", *Ph.D. thesis*, Georgia Institute of Technology, Atlanta, Georgia, U.S.A.

Mandal, P. and Calladine, C. R. (2002), "Lateral-Torsional Buckling of Beams and the Southwell Plot", *International Journal of Mechanical Sciences*, Vol. 44, No. 12, pp. 2557-2571.

Massey, C. (1963), "Elastic and Inelastic Lateral Instability of I-Beams", *The Engineer*, Vol. 216, No. 5622, pp. 672-674.

Meck, H. R. (1977), "Experimental Evaluation of Lateral Buckling Loads", *ASCE Journal of Engineering Mechanics Division, Proceedings*, Vol. 103, No. 2, pp. 331-337.

Southwell, E. V. (1932), "On the Analysis of Experimental Observations in Problems of Elastic Stability", *Proceedings of Royal Society of London*, Vol. 135, pp. 601-616.

Stratford, T. J. and Burgoyne, C. J. (1999), "Lateral Stability of Long Precast Concrete Beams", *Proceedings of the Institution of Civil Engineers: Structures and Buildings*, Vol. 134, No. 2, pp.169-180.

Trahair, N. S. (1969), "Deformations of Geometrically Imperfect Beams", *Proceedings of ASCE*, *Journal of Structural Division*, Vol. 95(ST7), pp.1475-1496.

Yura, J. A. (1970), Discussion of "Deformations of Geometrically Imperfect Beams" by Nicholas S. Trahair, *Journal of Structural Division*, *ASCE*, Vol. 96, No. 1, pp.162-163.

VI. REFERENCES

Allen, H. G. and Bulson, P. S. (1980), *Background to Buckling*, McGraw Hill, Maidenhead UK, p. 582.